Cold plasma copolymer with antimicrobial activity deposited on three different substrates

Erick Osvaldo Martínez Ruiz[1]* , Xi Rao[2] , Abril Fonseca García[1] ,
Carlos Gallardo Vega[1] , Carmen Natividad Alvarado Canche[1] , José Abraham Gonzáles López[1] ,
Antonio Serguei Ledezma Pérez[1] , Miriam Desiree Davila Medina[3] , Claudia Gabriela Cuellar Gaona[3] ,
Rosa Idalia Narro Céspedes[3] , Gustavo Soria Arguello[1] and María Guadalupe Neira Velázquez[1]*

1 Centro de Investigación en Química Aplicada, Saltillo, Coahuila, México
2 School of Materials and Energy, Southwest University of China, Chongqing, China
3 Facultad de Ciencias Químicas, Universidad autónoma de Coahuila, Saltillo, Coahuila de Zaragoza, México
*erickomr87@hotmail.com; *guadalupe.neira@ciqa.edu.mx

Abstract

A good strategy to prevent early deposition of bacteria that can form biofilms is the application of antimicrobial coatings to existing surfaces, however this field has been little explored and coatings are often non uniform in thickness. A homogeneous film of R-Carvone-Octadiene (ppCop) was deposited on different substrates (coverslip, minced coverslip and fabric) by cold plasma copolymerization to study the influence of the substrate on antimicrobial activity and show clues about the influence of octadiene on copolymerization. The ppCop showed better antimicrobial activity results on the substrate with higher effective contact area, highlighting the influence of this variable on antimicrobial activity. The ppCop deposited on minced coverslip showed an inhibition of *E. coli* and *S. aureus* bacteria by 48.69 ±0.08% and 49.31 ±0.58% respectively, with an average roughness of 14.1±0.02 nm and a static water contact angle of 79± 0.4°. The ppCop showed no cytotoxicity to the human cell line.

Keywords: *antimicrobial, biofilm, octadiene, plasma, R-Carvone.*

How to cite: Ruiz, E. O. M., Rao, X., García, A. F., Vega, C. G., Canche, C. N. A., López, J. A. G., Pérez, A. S. L., Medina, M. D. D., Gaona, C. G. C., Céspedes, R. I. N., Arguello, G. S., & Velázquez, M. G. N. (2023). Cold plasma copolymer with antimicrobial activity deposited on three different substrates. *Polímeros: Ciência e Tecnologia*, *33*(4), e20230038.

1. Introduction

It is well-known that bacterial biofilms are a major problem in different areas[1], despite the research efforts made in this field, it still remains a high priority in research. It has been found that up to 60% of infections treated are related to the formation of biofilms[2]. This problem is further aggravated by the emergence of bacteria with greater tolerance to biocides and antibiotics[3], in addition, in this state, the microorganisms are highly resistant to antimicrobial treatment and are tenaciously attached to the surface[4]. There are currently several innovative approaches focused on surface treatment to prevent this problem by improving the performance of existing antimicrobial surfaces, applying antimicrobial coatings, or modifying the surface architecture. Among surface modifications, the functionalization technique with chemicals, has been one of the most studied[1]. Cationic polymers, small ligands and biomolecules are reported to have the most successful antimicrobial activity and efficacy[5-8]. Most of the bactericidal surface modifications could exhibit cytotoxic properties to human cells. The durability of the chemical functionalization as well as its performance are usually limited and bacteria tend to develop tolerance in the case of leaching and non-leaching agents[9]. Another approach is surface topographical modification. This field

has been little explored and the influence of the topographic characteristics of the surface on its antimicrobial activity is still not fully understood and therefore it is an interesting field to explore. A significant advance in this field is that, contrary to what was thought, there is now sufficient evidence to document that there are bacteria capable of colonizing surfaces with average surface roughness (Ra) of the order of only few nanometers[10]. One of the most widely used methods for the prevention of biofilms on surfaces is the application of antimicrobial coatings, that can be defined as the deposition of an antimicrobial material on a substrate[11]. A commonly used strategy to obtain these coatings is the adhesion of an antimicrobial agent to a polymeric matrix. Examples that have been successfully reported include the use of Quaternary Ammonium Compounds (QACs) whose main antimicrobial activity is associated with their cation[12], nano-silver coatings have been widely used in medical devices, especially in catheters, however it is clear that silver ions and silver salts have potential cytotoxic properties for human cell lines[9]. Therefore, it would be appropriate to look for other alternatives that do not have this negative effect on humans and plasma treatment can be one of these alternatives. The concept of a diffusion layer to control the

Ruiz, E. O. M., Rao, X., García, A. F., Vega, C. G., Canche, C. N. A., López, J. A. G., Pérez, A. S. L., Medina, M. D. D., Gaona, C. G. C., Céspedes, R. I. N., Arguello, G. S., & Velázquez, M. G. N.

release of antibiotic like ciprofloxacin from a ciprofloxacin-loaded polyurethane by using n-butyl methacrylate plasma polymer has been studied[13]. Antimicrobial coatings are usually mechanically poor, non-uniform in thickness and in the case of coatings with release agents, the optimum concentration of the active ingredient decreases and with this also decreases its efficiency[11]. An alternative to obtain uniform antimicrobial coatings with acceptable mechanical properties is the use of cold plasma technology, which is used for the polymerization of organic precursors. Some monomers like trimethylsilane[14], 1,1,1 trichloroethane[15], R-carvone[16] and 1,8-cineole that is a natural monomer, were polymerized by plasma, and it was found that they have antibacterial properties[17]. One of the main advantages of the use of plasma polymerization is a great capacity to altering the surface chemistry without affecting the bulk properties of the material and with reproducible quality during manufacturing scale-up[18]. The main objective of the present work was the preparation of antibacterial coatings by means of plasma copolymerization of two organic precursors: essential oil known as R-carvone and octadiene. R-carvone essential oil (referred to in this work simply as carvone) is mainly extracted from spearmint plants and reported in the literature to possess antimicrobial properties[1,16,19-21]. These properties are mainly attributed to the presence of the monoterpene group present in its molecule[20]. This work highlights the influence of octadiene monomer in the study of the plasma "head-to-tail" copolymerization of R-carvone-octadiene monomer, under the hypothesis that by incorporating the -C_8H_{16}- group it acts as a "tail" to reduce the rigidity of the material and favor its roughness (modification of topographic characteristics). Since it has been reported that at higher values of roughness the hydrophobicity of the material is favored[22]. It is well-known that the hydrophobicity of a material is of great importance for the prevention of early deposition of bacteria that can form biofilms, thus conferring antimicrobial properties[23]. In this study, it was investigated, the antimicrobial activity of a cold plasma copolymer (ppCop) on three different substrates (coverslip, minced coverslip and fabric) under the Japanese Industrial Standard Z280126 protocol, exposing the importance of the surface area value of the substrate in the antimicrobial activity, whose influence has been little studied[11].

2. Materials and Methods

2.1. Cold plasma reactor for copolymerization reaction

A cylindrical glass container with stainless-steel caps was used as a plasma reactor as shown in Figure 1. The plasma reactor, by means of its stainless-steel caps, was connected to a 13.56 MHz radio frequency (RF) generator coupled with an impedance machine (model AT-6 Automatic Matching Network). The reactor was operated under vacuum conditions by the use of a vacuum pump (Maxima C Plus Fisher Scientific™). A single channel ACS 2000 adixen by Alcatel Vacuum Technology controller-indicator was used to read and monitor the vacuum pressure in the reactor. Prior to use of substrates for plasma copolymerization, such as glass coverslips, these were ultrasonically cleaned in acetone and milli-Q water, then dried, treated by air plasma for 1 min at
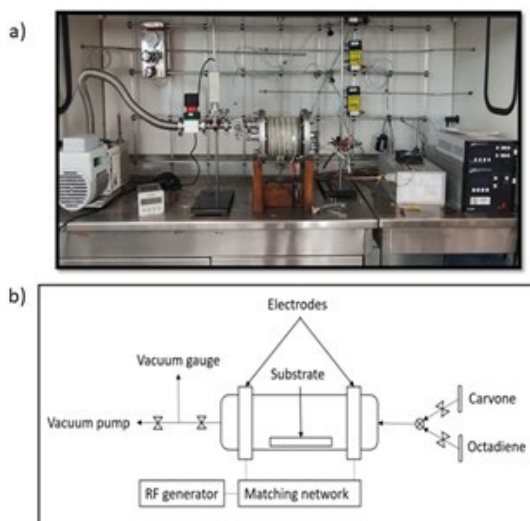
Figure 1. Experimental plasma reactor (a)) and plasma reactor scheme (b)).

20 W and 45 Pa to remove residual contaminants. Plasma copolymerization of carvone (98%, Sigma Aldrich product no.: 124931) and octadiene (98%, Sigma Aldrich product no.: O2501) was carried out on the 1 cm² substrates. The pressure data were used to obtain the corresponding flow rate (Q) by the use of the following Equation 1 (reported in standard cubic centimeters per minute, sccm)[23]:

$$Q = \left(\frac{dp}{dt}\right)\left(16172\frac{V}{T}\right) \qquad (1)$$

Where T=temperature (295 K), p = pressure (Pa), t = time (s) and V = volume of plasma reactor (1.65 L). The plasma reactor chamber was evacuated to reach a pressure of 38 Pa. Then the precursors (carvone oil and octadiene) were incorporated into the reactor at a flow rate of 0.9 and 0.5 sccm respectively. The plasma copolymerization was carried out at 20 W for 60 min of deposition. After plasma disruption the precursors continued to flow into the plasma chamber for another 2 min to quench any residual radicals on the ppCop.

2.2. Characterization techniques

All the experiments were repeated at least three times using three random samples deposited from three different cycles of plasma polymerization. The morphological and chemical techniques used for the study of the plasma polymerized R-carvone-octadiene (ppCop) include scanning electron microscopy (SEM), atomic force microscope (AFM), water contact angle (WCA), attenuated total reflection-Fourier transform infra-red (ATR-FTIR) and X-ray photoelectron spectroscopy (XPS). In the application of these methods, a coverslip was employed, onto which ppCop was deposited. The thermal stability of ppCop was evaluated by thermal gravimetric analysis (TGA). The cytotoxicity test on ppCop was assessed through 3- (4,5-dimethylthiazol-2-yl) -2,5-diphenyltetrazole bromide (MTT) assay using the primary human fibroblast cell line known as CCD-1064SK.

2.2.1. Roughness and thickness

The thickness of ppCop was measured with a surface profiler KLA Tencor (model: D-600) to determine the step height value of the sample. The step height was created by making a cross-section of the sample with a scalpel. The surface roughness of the ppCop was measured by an atomic force microscope (model: NEXT AFM NT-MDT). The AFM tip had a resonant frequency of 390 kHz and a constant force of 37 N/m. To measure average roughness (Ra) and root mean square roughness (Rq), scans were performed in areas of 5000 nm ×5000 nm on three different samples.

2.2.2. Static water contact angle (WCA)

The static water contact angle (WCA) of the coverslip deposited with ppCop was measured by the sessile drop technique. A ramé-hart equipment (model 100-00) was used to capture the WCA image and measured by the software Image J. To obtain the images, 2 μL of milli-Q water were manually dropped onto the sample for image captures. The commonly accepted range of WCA values for classification between hydrophobic and hydrophilic materials is 90°. The static WCA measurements were repeated on three different samples prepared by three separate cycles of plasma deposition.

2.2.3. Attenuated total reflection-Fourier transform infra-red (ATR-FTIR)

A Thermo Scientific ATR-FTIR system (Nicolet IS 50 ATR) was used to obtain the ppCop, octadiene and carvone spectrum. Once the ppCop was deposited on the coverslip and removed with a scalpel, this sample was used for the FTIR measurement. To obtain the spectra, 100 scans were performed at a resolution of 4 cm^{-1}.

2.2.4. X-ray photoelectron spectroscopy (XPS)

A ThermoFisher Thermo Scientific K-Alpha+ equipped with a monochromatic Al-Kα source (hv=1486.6 eV) operating at 25 W, 15 kV was used to obtain the XPS spectra corresponding to ppCop. Scanning spectra were collected at a step energy of 150 eV with a resolution of 1 eV, while high-resolution spectra were measured for C1s and N1s at a step energy of 50 eV with a resolution of 0.1 eV. The atomic concentration of nitrogen, oxygen and carbon were calculated thrice from the probe spectra with CasaXPS software. The high-resolution spectra were fitted by components with Origin 2019 software (version 2019 b). The C1s spectrum was subtracted with Shirley background and fitted by components with a half-width maximum (FWHM) of 1.35 eV, and a Gaussian component. Spectrum was also shifted according to the C-C and C-H components of the C1s peak at 284.48 eV. Relative sensitivity factors were provided by CasaXPS software.

2.3. Scanning electron microscopy (SEM)

Images of the different samples of fabric and coverslip deposited by ppCop have been collected with Scanning Electron Microscopy (SEM), JEOL 6000 apparatus. The samples with ppCop were previously coated with a 10 nm layer of gold by plasma sputtering system and mounted on aluminum stubs.

2.4. Thermal gravimetric analysis (TGA)

Thermogravimetric analysis was performed using a TGA-Q500-V6.7 equipment, using open pans under dry nitrogen atmosphere (nitrogen flow of 100 mL/min), and at 600 °C oxygen was injected (50 mL/min) into the chamber to enhance the oxidation process. Measurements were performed by increasing the temperature from room temperature up to 600 °C at 10 °C/min and from 600 up to 700 at 20 °C/min. To collect the sample, a scalpel was utilized to carefully detach the film from the coverslip. The film was then transferred and stored in a petri dish to facilitate subsequent TGA analysis. The mass-temperature derivative (MTD) was acquired, enabling a more detailed examination of the distinct stages involved in the decomposition processes. It is noteworthy to mention that the transition to an oxygen atmosphere was implemented to ensure the absence of non-organic impurities in the studied sample, such as potential remnants of coverslip that could be present due to the method of sample collection.

2.5. Antimicrobial activity of copolymer

The antimicrobial activity of ppCop was evaluated based on the Japanese Industrial Standard, Z280126[24]. The evaluation was conducted using two clinically important microorganisms: *Escherichia coli* ATCC-25922 and *Staphylococcus aureus* ATCC-29213. To perform the test, fabrics and coverslips coated with ppCop (each having a circular shape with a diameter of 1.75 cm) were prepared under aseptic conditions. These samples were then inoculated with 4 mL of a suspension containing the microorganisms in trypticase soy broth. The concentration of the suspension was equivalent to 50,000 colony-forming units per mL (CFU mL^{-1}). Additionally, a third set of coverslips minced (approximately 0.1 g, equivalent to a coverslip of 1.75 of diameter) coated with ppCop was treated in the same manner as the previous samples. Afterward, the samples were incubated in a controlled environment with a temperature of 37 °C and humidity maintained at 90% for a duration of 24 hr. Following the incubation period, one part of the inoculum (1 x 10^6 CFU mL^{-1}) was combined with nine parts of mQ water to prepare an inoculum concentration of 1 x 10^5 CFU mL^{-1}. This mixture was further diluted to achieve an inoculum concentration of 1 x 10^2 CFU mL^{-1}. Each dilution was then added to a petri dish containing 20 mL of agar BD BIOXON (model BD210800). The petri dishes were left at a temperature of 37 °C for 24 hr. After this incubation period, the colony-forming units (CFUs) were counted with a microscope for each sample as well as the control. The methodology described above was carried out in triplicate for each treated sample, chosen from three different cycles of plasma treatment. Once the UFCs of each sample were determined, the antimicrobial activity (R) was calculated using the Equation 2.

$$R = Log\left(\frac{B_0}{M_t}\right) \tag{2}$$

Where B$_0$ is the quantity in CFU mL^{-1} of bacteria that survive in the presence of the blank (coverslip without ppCop) after 24 hours of incubation. M$_t$ is the number of bacteria

Ruiz, E. O. M., Rao, X., García, A. F., Vega, C. G., Canche, C. N. A., López, J. A. G., Pérez, A. S. L., Medina, M. D. D., Gaona, C. G. C., Céspedes, R. I. N., Arguello, G. S., & Velázquez, M. G. N.

that survive after 24 hr of incubation in the presence of the ppCop. Additionally, bacterial growth inhibition (GI) was determined by Equation 3.

$$GI = \left(\frac{B_0 - M_t}{B_0} \right) *100 \qquad (3)$$

2.6. Hemolysis and In vitro cytotoxicity test: MTT assays

The hemolysis tests were performed with freshly human blood collected from non-smoking volunteer donors. The blood was collected in heparinized tubes and centrifuged at 3000 rpm for 4 min at 4 °C. The sediment obtained was washed three times with cold Alsever solution (AS) consisting of dextrose 0.116 M, sodium chloride 0.071 M, sodium citrate 0.027 M and citric acid 0.002 M. The supernatant was diluted at 1:99 with Alsever solution. Subsequently, 150 µL of this suspension was taken for experiments. This red blood cell (RBC) solution was used within 24 hours after collection. The samples were prepared at concentrations of 1, 2.5 and 5 mg mL^{-1}. The tubes were gently mixed on a rotary shaker and incubated at 36.5 °C in a shaking water bath for 1 hour. Alsever solution and deionized water were used as negative and positive controls, respectively. Samples were centrifuged at 2500 rpm for 4 min and free hemoglobin in the supernatant was measured spectrophotometrically by UV at 415 nm (Sinergy HTX model). The percentage of hemolysis was measured using the following Equation 4:

$$\%HE = \left(\frac{A_s - A_{cn}}{A_{cn} - A_{cp}} \right) *100 \qquad (4)$$

Where %HE is the percentage of hemolysis, As is the absorbance of the sample, Acn is the absorbance of the negative control and Acp is the absorbance of the positive control. For cytotoxicity evaluation, the MTT test was performed on the ppCop film at 1 and 3 days in accordance with the ISO standard 10993[25], the well (polyethylene) without ppCop in which cells were cultured was used as a control. The cells used were the human fibroblast cell line CCD-1064SK.

3. Results and Discussions

3.1. Aging test

Samples of the ppCop were immersed in mQ water and dimethyl sulfoxide (DMSO) for 24 hours as a material aging test. The results obtained are shown in Table 1. Considering the negligible reduction (0.5%) in ppCop thickness in dimethyl sulfoxide (DMSO) it is likely that the current deposition condition confers a high degree of cross-linking to ppCop to prevent its dissolution in DMSO[26]. On the other hand, the almost negligible reduction of ppCop thickness in mQ water, thus ppCop can be considered to be stable in water.

Based on the results of Figure 2, it is possible to observe the 2D and 3D AFM images of ppCop roughness, the ppCop shows an average roughness (Ra) of 14.1±0.02 nm and root mean square roughness (Rq) of 17.1±0.02 nm. The relatively high values of roughness are possibly due to the long plasma copolymerization time (1 hour) and the insertion of groups -C$_8$H$_{16}$- in the ppCop, which can act as a flexible tail that facilitates the rough structure of the material[22].

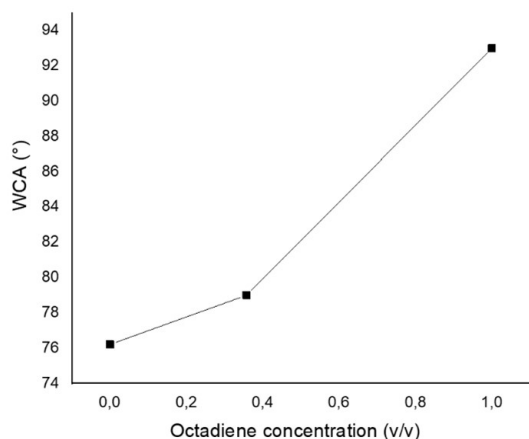### 3.2. Static water contact angle (WCA)

Plasma polymerizations were performed at the same ppCop operating conditions (1.4 sccm, 20 W and 60 min) for carvone (octadiene concentration = 0 v/v) and octadiene (carvone concentration = 0 v/v) monomers. Figure 3 shows the behavior of the WCA as a function of the octadiene concentration used for polymerization. Is shown a WCA value for ppCop (octadiene concentration =0.357 v/v) of 79± 0.4°. It is observed that the WCA value increases as the octadiene concentration increases, this can be explained by the chemical nature of the monomer, in whose molecular

Table 1. Thickness of ppCop as deposited and after immersed in mQ water and DMSO.

	Thickness (nm)
ppCop as deposited	857.2 ±29.5
24 h mQ water immersed	855.3 ±33.4
24 h Dimethyl Sulfoxide (DMSO)	852.6 ±27.3
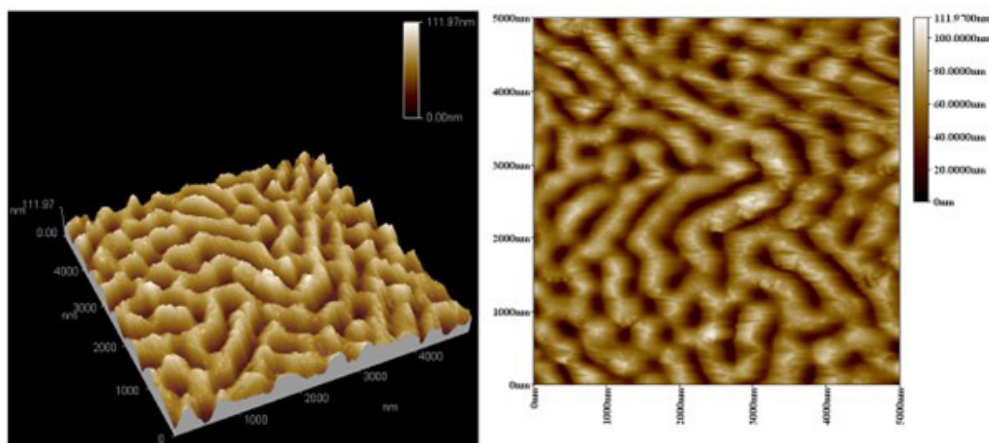
Figure 2. 3D and 2D AFM image roughness morphology of ppCop, scan size: 5000 nm ×5000 nm.

Figure 3. WCA static water contact angle as a function of octadiene concentration in the polymer obtained by cold plasma polymerization.

Figure 4. ATR-FTIR spectra of ppCop, octadiene and carvone.

Figure 5. Survey spectra for ppCop (pass energy of 150 eV with a resolution of 1 eV).

structure there is no oxygen available to find OH⁻ group in the plasma polymerization. The OH⁻ group is the main responsible for hydrophilicity of surfaces[27]. The opposite behavior occurs if we observe the concentration of carvone, in whose molecule there is oxygen available for the eventual appearance of the OH⁻ group on the surface of the plasma polymerization. The static WCA of the clean glass coverslip (positive control) was $21.6 \pm 0.6°$. This behavior may be due to the silanol groups present on the coverslip[16].

Since hydrophobicity of a material is of great importance for the prevention of early deposition of bacteria that can form biofilms[28]. Similar results can be found in the literature for the WCA values of plasma polymerizations of carvone and octadiene[16]. However, a better antimicrobial activity is reported in the polymerization of carvone compared to that of octadiene, attributing the influence on the antimicrobial activity to the oxidizing groups in the polymeric film obtained from carvone.

### 3.3. Attenuated total reflection Fourier transform infrared (ATR-FTIR)

The present technique identifies the functional groups on the surface of ppCop and provides clues regarding to its copolymerization route on the coverslip.

In Figure 4 it is possible to observe the ATR-FTIR spectra of ppCop, octadiene and carvone oil. The ppCop spectra showed broad bands with respect to its precursors which showed regular sharp bands, this is a characteristic of a highly crosslinked polymer[29]. In the system under investigation in this study, both carvone and octadiene exhibit terminal double bonds within their chemical structures, thereby possessing the potential for polymerization. Octadiene showcases the presence of two terminal double bonds, effectively yielding four reactive centers. Consequently, the resulting copolymer may display the phenomenon of cross-linking[30].

Highly cross-linked polymers like ppCop could reduce the intensity of the symmetric structure of moieties like CH_3 at 1371 cm⁻¹[29]. The considerable reduction of the =CH bond (990.28 and 908.80 cm⁻¹) and stretch bonds (3079.33 cm⁻¹)
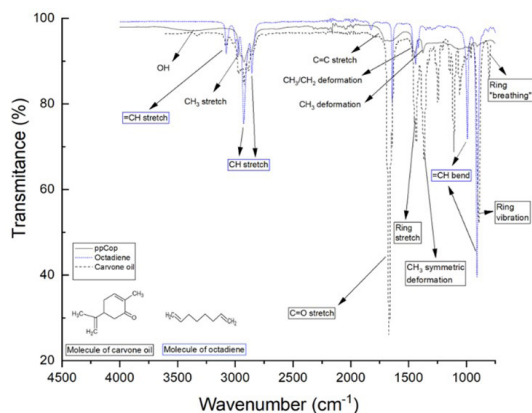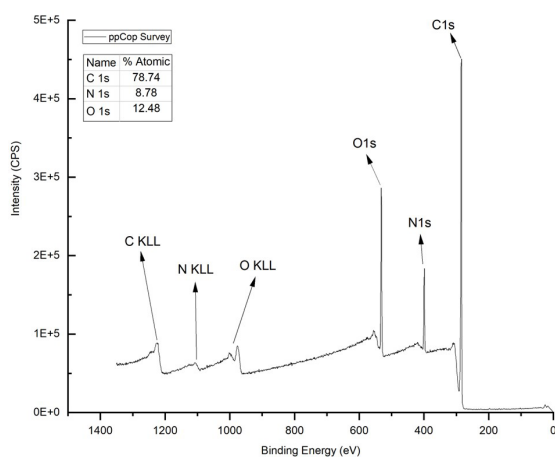
suggests that the copolymerization also is carried out by the =CH bond of octadiene. This suggests the insertion of long chain hydrocarbons such as $-C_8H_{16}-$, which could give flexibility to the polymer and increase its roughness as discussed previously in section 3.1.

However, the ring stretch, vibration and "breathing" (i.e., simultaneous stretch of all C=C bonds) of carvone oil at 1430.61, 893.70 and 802.20 cm⁻¹ were missing from the IR spectra of the ppCop[30,31]. This absence suggested that the ring structure of carvone, as illustrated in Figure 4 is dissociated during their plasma copolymerization on the coverslip substrate[16].

3.4. X-ray photoelectron spectroscopy (XPS)

In Figure 5 are presented the XPS atomic compositions and functional groups for ppCop film (upper 10 nm of its surface). Elements such as C (78.74%, 284.08 eV), N (8.78%, 399.08 eV) and O (12.48%, 532.08 eV) were identified. The presence of N in the deposited film is probably caused by residual air nitrogen in the plasma reactor, which was ionized and participated in the copolymerization mechanism.

Similar cases of nitrogen presence have been reported for plasma-treated polymeric substrates[16].

The percentages of the types of chemical bonds (C1s) studied in the procedure as are illustrated in Figure 6, were the following; C1 (C-H/C-C corresponding to 284.48 eV) 73.27%, C2 (C-O-C/C-N/C-OH at 286.05 eV) 16.61%, C3 (N-C = O, C = O at 287.55) 9.35% and C4 (O-C = O at 289.1 eV) 0.76%. The N/C and O/C ratios on the surface of the film were 0.12 and 0.16 respectively. The relative
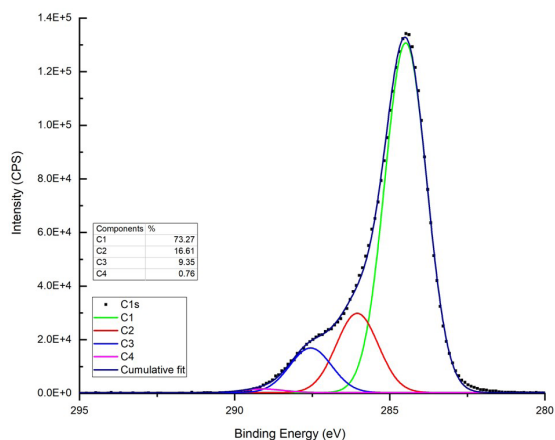
abundance of N in the film could have an influence on the relative low hydrophobicity of the material by hydrogen bonding in an aqueous medium. In the literature it can be found that oxidizing groups, especially carbonyl, are responsible for the antibacterial activity of the plasma coating film. In the results obtained by XPS, it was found that the oxidant groups C3 and C4 correspond in total to 10.1% on the surface of the ppCop. Specifically, carbonyl and N-C = O have a presence of 9.35%.
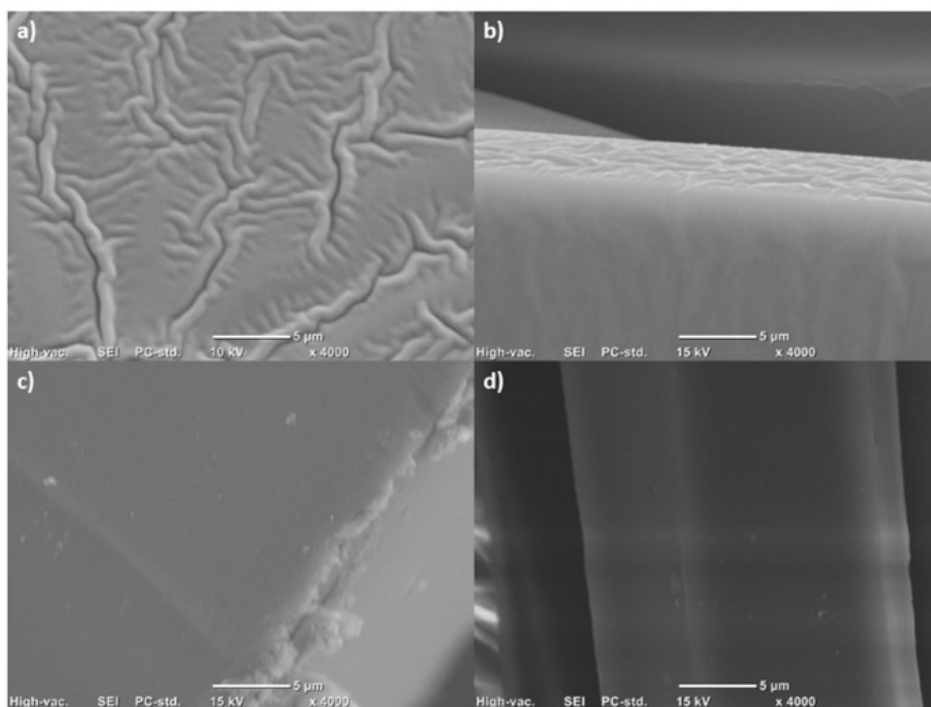
3.5. Scanning electron microscope (SEM)

Figure 7 shows the SEM images of ppCop on coverslips (a) and tissue (b), as well as the uncoated coverslip and tissue (c) and d) respectively). It is possible to observe a homogeneous rough deposit on both substrates, these images reinforce the evidence of the roughness of ppCop. It is appreciated that the plasma coating was homogeneously deposited on the two substrates. Similar morphology was found in the literature in plasma polymerized methyl acrylate coatings of comparable thickness and same elements present (C, O and H) as in ppCop. The appearance of folding/ agglomeration is possibly due to structural accommodations in the polymer formation during the plasma polymerization process, resulting in different mass percentages of C, O and H in the coating at different film thicknesses[32]. However, further studies are needed to confirm this.

Figure 6. Component-fitted C1s spectra for ppCop as deposited, C1 (C-H / C-C), C2 (C-O-C / C-N / C-OH), C3 (N-C = O, C = O) and C4 (O-C = O).

3.6. Thermal gravimetric analysis (TGA)

As shown in Figure 8, it was possible to see the weight loss of the ppCop sample (initial weight of 3.135 mg) as a

Figure 7. SEM images of ppCop on coverslips (a) and tissue (b), as well as the uncoated coverslip and tissue (c) and d) respectively), scale bar of 5 μm.

function of temperature (from room temperature, and up to 700 °C) and its associated MTD. The TGA curve for the ppCop polymer shows that the polymer begins to degrade from 100 ˚C, and this process ends around 475 °C. In the MTD curve, it can be seen that the polymer follows a two-stage decomposition kinetics, a shoulder is observed in the first stage around 250°C and a peak is also observed at a temperature of 375°C, indicating that the copolymer degrades in two stages, it is possible that each one of the two signals correspond to each of the monomers of the copolymer (ppCop), which was synthesized from two monomers (octadiene and carvone)[33]. In the thermogram, it can also be seen that around 475 ˚C, about 10% residue remains, which could be due to the presence of crosslinked polymer[34]. The sample maintains this percentage without significant change until oxygen is introduced at 600 °C, leading to its complete oxidation.

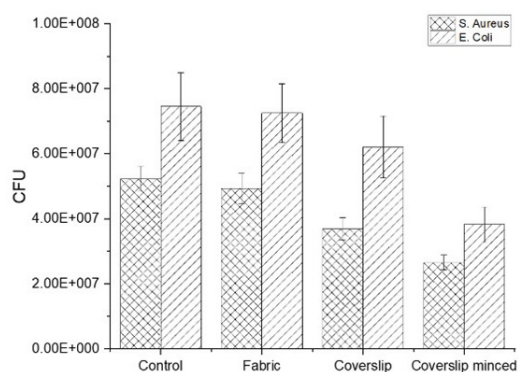### 3.7. Antimicrobial activity of copolymer

In Figure 9 it is possible to observe the CFUs in presence of ppCop on three different substrates (fabric, coverslip and minced coverslip) and the substrate without ppCop (control) after 24 hr of bacteria growth (*S.aureus* and *E. coli*). The results present inhibition in the growth of the CFU respect to the control. The most significant inhibition in the bacteria growth is reported in the ppCop deposited on the minced coverslip (48% for *E. coli* and 49% for *S. aureus*), followed by the ppCop deposited on the coverslip (16% for *E. coli* and 29% for *S. aureus*) and finally the fabric with only an inhibition of 3% and 6% for *E. coli* and *S. aureus* respectively. The inhibition in CFU could be mainly due

to the hydrophobicity of the material and the presence of oxidizing groups, such as carbonyl in the ppCop which correspond to 9.35% of the surface of ppCop according to the data obtained by XPS.

Antimicrobial activity (R) and bacterial growth inhibition (GI) of the ppCop deposited on three different substrates (fabric, coverslip and minced coverslip) it is shown in Table 2. The highest values in antimicrobial activity (R) are present in the ppCop deposited on minced coverslip with 0.29 ±0.007 for *E. coli* and 0.29±0.004 for *S. aureus*, followed by the ppCop deposited on coverslip with 0.079 ±0.004 for *E. coli* and 0.15±0.007 for *S. aureus* and finally the ppCop deposited on fabric with only 0.012 ±0.005 and 0.025±0.009 for *E. coli* and *S. aureus* respectively. This behavior, can be attributed to the different effective contact areas in the three different substrates, which is greater in the minced coverslip, followed by the coverslip and less in the fabric. It is important to mention that these bacteria measure approximately 0.5 µm wide by 2 µm long in the case of *E. coli* and 1.5 µm in diameter for *S. Aureus* which is considered immobile. The dimensions of the bacteria used limit the effective contact area to dimensions greater than approximately 4 µm² of surface, this represents a difficulty in establishing an effective contact of the bacteria in the ppCop deposited on fabric since this type of substrate is characteristic for having a morphology with irregularities of dimensions smaller than the size of bacteria. This fact, together with the inability of the bacteria to migrate to these irregularities in the matrix due to their little or no immobility (in the case of *S. aureus*), difficulties the effective contact
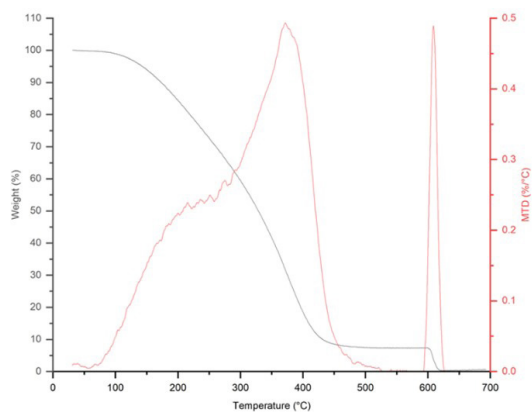

Figure 8. TGA thermogram of ppCop (initial sample weight of 3.135 mg).

Figure 9. CFU in presence of ppCop on three different substrates (fabric, coverslip and minced coverslip) and without presence of ppCop (control) at 24 hr of bacteria growth (*S. aureus* and *E. coli*).

Table 2. Antimicrobial activity (R) and bacterial growth inhibition (GI) of the ppCop deposited on three different substrates (fabric, coverslip and minced coverslip).

| | *Escherichia coli* | | *Staphylococcus aureus* | |
	R	**GI (%)**	**R**	**GI (%)**
Fabric	0.012 ±0.005	2.71 ±1.3	0.025±0.009	5.76 ±2
Coverslip	0.079 ±0.004	16.72 ±0.93	0.15±0.007	29.57 ±1.29
Minced coverslip	0.29 ±0.007	48.69 ±0.08	0.29±0.004	49.31 ±0.58
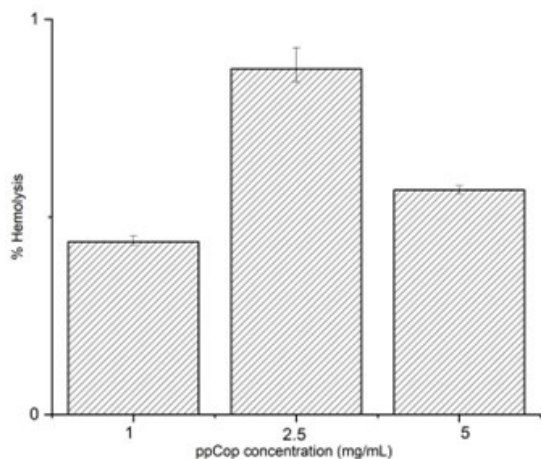
Figure 10. Percentage of hemolysis at three different concentrations (1, 2.5 and 5 mg mL^{-1}) of ppCop.

Figure 11. Percentage of cell viability (human CCD-1064SK fibroblasts) for ppCop at 1 and 3 days of culture.

of the bacteria with the ppCop and decreasing the value of GI on this matrix.

Comparable materials to ppCop have been reported in the literature, the plasma polymerization of Octadiene (ppOct) with antibacterial properties was found. The microbial activity (R) for this ppOct is reported equal to 0.39 for *S. aureus* and 0.34 for *E. coli* reporting a inhibition in bacteria population of 60% and 55% for *S. aureus* and *E. coli* respectively[16]. The difference in antimicrobial activity in both materials is possible due to the reported hydrophobic properties of the polymer. In the case of ppOct, is reported a value of 92.9 ± 0.9°[16] and ppCop of 79 ± 0.4°. Since ppOct is more hydrophobic than ppCop has a higher repulsive effect on the initial bacteria attached which promotes a higher antimicrobial activity[28]. Nevertheless, the antimicrobial activity is comparable between both materials when ppCop is deposited on the ground coverslip. This could be attributed to the presence of oxidant groups (C3 + C4 equal to 10.11% according to XPS analysis) on the surface of the ppCop that are reported in a much lower amount in the ppOct (only C3 equal to 2.7%). The presence of these oxidant groups could lead to the deterioration of the bacteria and therefore favor the antimicrobial activity[1].

3.8. Hemolysis and cytotoxicity test: MTT assays

The results of the %HE at three different concentrations of ppCop (1, 2.5 and 5 mg mL^{-1}) are presented in Figure 10. It can be observed that ppCop does not exceed the value of 2 of % Hemolysis (HE) in any of the three different concentrations. Therefore, and considering the standard ASTM F 756 17[35], it was found that ppCop does not present hemolytic activity. These results suggest that the material studied could be used for applications where there is direct interaction with human blood.

In Figure 11 is showed that the material has an acceptable viability according to the ISO 10993-5 standard[25] (established a minimum of 70%) on day 3, since on day 1 a viability of 54.94 ± 1.69% was shown, while for day 3 the viability was 90.42 ± 3.10%. These results support the hypothesis that the plasma coating material is not cytotoxic for the human
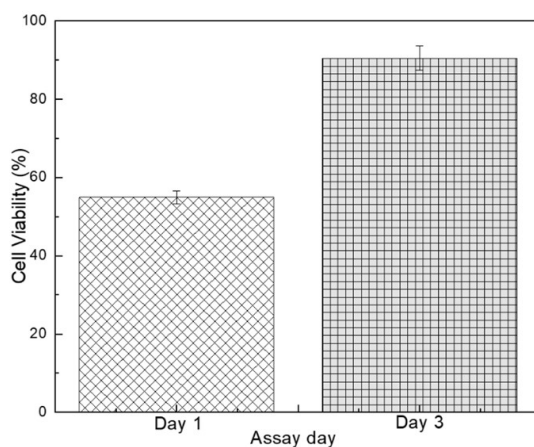
cell line tested, which makes it possible for this material to be used for applications in which there is interaction with (human) body tissues.

4. Conclusions

A cold plasma copolymerization of R-carvone and Octadiene was performed to obtain a moderately hydrophobic copolymer (ppCop) (WCA = 79± 0.4°). XPS analysis showed that ppCop was a typical cross-linked hydrocarbon plasma polymer with presence of carboxyl, amine-amide and hydroxyl moieties on the surfaces. The almost negligible reduction of ppCop thickness in DMSO (only reduced by 0.5%) during the 24 h immersion in DMSO reinforces the hypothesis that the ppCop is a cross-linked copolymer. The considerable reduction of the =CH bond (990.28 and 908.80 cm^{-1}) and stretch bonds (3079.33 cm^{-1}) of octadiene and the relatively high values of roughness (Ra of 14.1±0.02 nm and Rq of 17.1±0.02 nm) may suggest the insertion of long chain hydrocarbons such as -C$_8$H$_{16}$-, which could give flexibility to the polymer and increase its surface roughness. However, additional studies are needed to confirm this. The thermal stability of the ppCop was reported by the performance of Thermal gravimetric analysis (TGA). The thermal degradation of the sample initiated at 100 °C, it can be seen that the polymer follows a two-stage decomposition kinetics possibly attached to the copolymeric nature of the material. Approximately 10 percent of the initial sample weight was retained until the final oxidation occurred at 600 °C under an oxygen atmosphere, which could be due to the presence of crosslinked polymer. Antimicrobial activity of ppCop was corroborated by favorable outcomes observed in three different substrates (coverslip, minced coverslip and fabric), with the minced coverslip substrate displaying the highest value of growth inhibition (GI) with 48.69 ± 0.08% inhibition of *E. coli* and 49.31 ± 0.58% inhibition of *S. aureus*. The lowest GI result was for the fabric substrate reporting results of 2.71 ± 1.3% inhibition of *E. coli* and 5.76 ± 2% of inhibition of *S. aureus*, highlighting the influence of the effective contact area of each substrate

on the GI and therefore microbial activity. Lastly, ppCop showed no cytotoxicity effect towards human cell during the hemolysis and cell adhesion assay.

5. Author's Contribution

• **Conceptualization** – Erick Osvaldo Martínez Ruiz; María Guadalupe Neira Velázquez.

• **Data curation** – José Abraham Gonzáles López; Erick Osvaldo Martínez Ruiz; Carlos Gallardo Vega.

• **Formal analysis** – Erick Osvaldo Martínez Ruiz; Carlos Gallardo Vega; José Abraham Gonzáles López.

• **Funding acquisition** – María Guadalupe Neira Velázquez; Rosa Idalia Narro Céspedes.

• **Investigation –** Erick Osvaldo Martínez Ruiz; Xi Rao; Carmen Natividad Alvarado Canche; Claudia Gabriela Cuellar Gaona; Abril Fonseca García; Miriam Desiree Davila Medina; José Abraham Gonzáles López; Gustavo Soria Arguello.

• **Methodology** – Erick Osvaldo Martínez Ruiz.

• **Project administration** –Erick Osvaldo Martínez Ruiz; María Guadalupe Neira Velázquez.

• **Resources** – María Guadalupe Neira Velázquez; Xi Rao; Antonio Serguei Ledezma Pérez; Miriam Desiree Davila Medina; Rosa Idalia Narro Céspedes.

• **Software** – Erick Osvaldo Martínez Ruiz; Carlos Gallardo Vega.

• **Supervision** – Erick Osvaldo Martínez Ruiz; María Guadalupe Neira Velázquez.

• **Validation** – Erick Osvaldo Martínez Ruiz; María Guadalupe Neira Velázquez; Antonio Serguei Ledezma Pérez; Claudia Gabriela Cuellar Gaona; Carmen Natividad Alvarado Canche; Abril Fonseca García.

• **Visualization** – Erick Osvaldo Martínez Ruiz; María Guadalupe Neira Velázquez.

• **Writing – original draft** – Erick Osvaldo Martínez Ruiz; María Guadalupe Neira Velázquez.

• **Writing – review & editing** – Erick Osvaldo Martínez Ruiz; María Guadalupe Neira Velázquez.

6. Acknowledgements

7. References

1. Carvalho, C. C. C. R., & Fonseca, M. M. R. (2007). Preventing biofilm formation: promoting cell separation with terpenes. *FEMS Microbiology Ecology*, *61*(3), 406-413. http://dx.doi.org/10.1111/j.1574-6941.2007.00352.x. PMid:17617221.

2. Fux, C. A., Costerton, J. W., Stewart, P. S., & Stoodley, P. (2005). Survival strategies of infectious biofilms. *Trends in Microbiology*, *13*(1), 34-40. http://dx.doi.org/10.1016/j.tim.2004.11.010. PMid:15639630.

3. Bahrami, A., Delshadi, R., & Jafari, S. M. (2020). Active delivery of antimicrobial nanoparticles into microbial cells through surface functionalization strategies. *Trends in Food Science & Technology*, *99*, 217-228. http://dx.doi.org/10.1016/j.tifs.2020.03.008.

4. Donlan, R. M. (2001). Biofilms and device-associated infections. *Emerging Infectious Diseases*, *7*(2), 277-281. http://dx.doi.org/10.3201/eid0702.010226. PMid:11294723.

5. Sunil, B. R., Kiran, A. S. K., & Ramakrishna, S. (2022). Surface functionalized titanium with enhanced bioactivity and antimicrobial properties through surface engineering strategies for bone implant applications. *Current Opinion in Biomedical Engineering*, *23*, 100398. http://dx.doi.org/10.1016/j.cobme.2022.100398.

6. Bouzaheur, A., Bouchoucha, A., Larbi, K. S., & Zaater, S. (2022). Experimental and DFT studies of a novel Schiff base sulfonamide derivative ligand and its palladium (II) and platinum (IV) complexes: antimicrobial activity, cytotoxicity, and molecular docking study. *Journal of Molecular Structure*, *1261*, 132811. http://dx.doi.org/10.1016/j.molstruc.2022.132811.

7. Xu, Q., He, P., Wang, J., Chen, H., Lv, F., Liu, L., Wang, S., & Yoon, J. (2019). Antimicrobial activity of a conjugated polymer with cationic backbone. *Dyes and Pigments*, *160*, 519-523. http://dx.doi.org/10.1016/j.dyepig.2018.08.049.

8. Aslam, M., Abdullah, A. Z., & Rafatullah, M. (2021). Recent development in the green synthesis of titanium dioxide nanoparticles using plant-based biomolecules for environmental and antimicrobial applications. *Journal of Industrial and Engineering Chemistry*, *98*, 1-16. http://dx.doi.org/10.1016/j.jiec.2021.04.010.

9. Knetsch, M. L. W., & Koole, L. H. (2011). New Strategies in the Development of Antimicrobial Coatings: The Example of Increasing Usage of Silver and Silver Nanoparticles. *Polymers*, *3*(1), 340-366. http://dx.doi.org/10.3390/polym3010340.

10. Truong, V. K., Lapovok, R., Estrin, Y. S., Rundell, S., Wang, J. Y., Fluke, C. J., Crawford, R. J., & Ivanova, E. P. (2010). The influence of nano-scale surface roughness on bacterial adhesion to ultrafine-grained titanium. *Biomaterials*, *31*(13), 3674-3683. http://dx.doi.org/10.1016/j.biomaterials.2010.01.071. PMid:20163851.

11. Hasan, J., Crawford, R. J., & Ivanova, E. P. (2013). Antibacterial surfaces: the quest for a new generation of biomaterials. *Trends in Biotechnology*, *31*(5), 295-304. http://dx.doi.org/10.1016/j.tibtech.2013.01.017. PMid:23434154.

12. Hegstad, K., Langsrud, S., Lunestad, B. T., Scheie, A. A., Sunde, M., & Yazdankhah, S. P. (2010). Does the wide use of quaternary ammonium compounds enhance the selection and spread of antimicrobial resistance and thus threaten our health? *Microbial Drug Resistance (Larchmont, N.Y.)*, *16*(2), 91-104. http://dx.doi.org/10.1089/mdr.2009.0120. PMid:20370507.

13. Kwok, C. S., Horbett, T. A., & Ratner, B. D. (1999). Design of infection-resistant antibiotic-releasing polymers. II. Controlled release of antibiotics through a plasma-deposited thin film barrier. *Journal of Controlled Release*, *62*(3), 301-311. http://dx.doi.org/10.1016/S0168-3659(99)00105-4. PMid:10528068.

14. Ma, Y., Chen, M., Jones, J. E., Ritts, A. C., Yu, Q., & Sun, H. (2012). Inhibition of Staphylococcus epidermidis biofilm by trimethylsilane plasma coating. *Antimicrobial Agents and Chemotherapy*, *56*(11), 5923-5937. http://dx.doi.org/10.1128/AAC.01739-12. PMid:22964248.

15. Michl, T. D., Coad, B. R., Doran, M., Hüsler, A., Valentin, J. D. P., Vasilev, K., & Griesser, H. J. (2014). Plasma polymerization

Ruiz, E. O. M., Rao, X., García, A. F, Vega, C. G., Canche, C. N. A., López, J. A. G., Pérez, A. S. L., Medina, M. D. D., Gaona, C. G. C., Céspedes, R. I. N., Arguello, G. S., & Velázquez, M. G. N.

of 1,1,1-trichloroethane yields a coating with robust antibacterial surface properties. *RSC Advances*, *4*(52), 27604-27606. http://dx.doi.org/10.1039/C4RA01892C.

16. Chan, Y. W., Siow, K. S., Ng, P. Y., Gires, U., & Majlis, B. Y. (2016). Plasma polymerized carvone as an antibacterial and biocompatible coating. *Materials Science and Engineering C*, *68*, 861-871. http://dx.doi.org/10.1016/j.msec.2016.07.040. PMid:27524089.

17. Pegalajar-Jurado, A., Easton, C. D., Styan, K. E., & McArthur, S. L. (2014). Antibacterial activity studies of plasma polymerised cineole films. *Journal of Materials Chemistry. B, Materials for Biology and Medicine*, *2*(31), 4993-5002. http://dx.doi.org/10.1039/C4TB00633J. PMid:32261832.

18. Chu, P. K., Chen, J. Y., Wang, L. P., & Huang, N. (2002). Plasma-surface modification of biomaterials. *Materials Science and Engineering R Reports*, *36*(5-6), 143-206. http://dx.doi.org/10.1016/S0927-796X(02)00004-9.

19. Aggarwal, K. K., Khanuja, S. P. S., Ahmad, A., Kumar, T. R. S., Gupta, V. K., & Kumar, S. (2002). Antimicrobial activity profiles of the two enantiomers of limonene and carvone isolated from the oils ofMentha spicata andAnethum sowa. *Flavour and Fragrance Journal*, *17*(1), 59-63. http://dx.doi.org/10.1002/ffj.1040.

20. Carvalho, C. C. C. R., & Fonseca, M. M. R. (2006). Carvone: why and how should one bother to produce this terpene. *Food Chemistry*, *95*(3), 413-422. http://dx.doi.org/10.1016/j.foodchem.2005.01.003.

21. Castiglione, K., Fu, Y., Polte, I., Leupold, S., Meo, A., & Weuster-Botz, D. (2017). Asymmetric whole-cell bioreduction of (R)-carvone by recombinant Escherichia coli with in situ substrate supply and product removal. *Biochemical Engineering Journal*, *117*(Pt A), 102-111. http://dx.doi.org/10.1016/j.bej.2016.10.002.

22. An, T., Deng, X., Liu, S., Wang, S., Ju, J., & Dou, C. (2018). Growth and roughness dependent wetting properties of CeO2 films prepared by glancing angle deposition. *Ceramics International*, *44*(8), 9742-9745. http://dx.doi.org/10.1016/j.ceramint.2018.02.206.

23. Yasuda, H. K. (1985). *Plasma polymerization*. USA: Academic Press.

24. Japan Standard Association - JSA. JIS Z 2801:2000: Antimicrobial products—Test for antimicrobial activity and efficiency. Japan: Japan Standard Association; 2000.

25. International Organization for Standardization – ISO. ISO 10993-5:2009 Biological evaluation of medical devices — Part 5: Tests for in vitro cytotoxicity. Switzerland: ISO; 2009.

26. Chan, Y. W., Chen, T. F., Siow, K., Majlis, B. Y., & Yeoh, T. S. (2015). *TRIZ technique to produce stable plasma modified surfaces with high density of reactive chemical functionalities.* In *2015 IEEE Conference on Sustainable Utilization And Development In Engineering and Technology (CSUDET)* (pp. 1-6). Selangor, Malaysia: IEEE. http://dx.doi.org/10.1109/CSUDET.2015.7446218

27. Nambafu, G. S., Kim, N., & Kim, J. (2022). Hydrophobic coatings prepared using various dipodal silane-functionalized polymer precursors. *Applied Surface Science Advances*, *7*, 100207. http://dx.doi.org/10.1016/j.apsadv.2021.100207.

28. Ong, Y.-L., Razatos, A., Georgiou, G., & Sharma, M. M. (1999). Adhesion forces between E. coli bacteria and biomaterial surfaces. *Langmuir*, *15*(8), 2719-2725. http://dx.doi.org/10.1021/la981104e.

29. Siow, K. S., Britcher, L., Kumar, S., & Griesser, H. J. (2014). Deposition and XPS and FTIR analysis of plasma polymer coatings containing phosphorus. *Plasma Processes and Polymers*, *11*(2), 133-141. http://dx.doi.org/10.1002/ppap.201300115.

30. Odian, G. (2004). *Principles of polymerization*. USA: John Wiley & Sons.. http://dx.doi.org/10.1002/047147875X.

31. Lin-Vien, D., Colthup, N. B., Fateley, W. G., & Grasselli, J. G. (1991). *The Handbook of infrared and raman characteristic frequencies of organic molecules*. Boston: Academic Press.

32. Nath, S. D., & Bhuiyan, A. H. (2023). Surface morphology and optical properties of thin films of plasma polymerized methyl acrylate. *Optical Materials*, *136*, 113474. http://dx.doi.org/10.1016/j.optmat.2023.113474.

33. Dey, A., Mete, S., Banerjee, S., Haldar, U., Rajasekhar, T., Srikanth, K., Faust, R., & De, P. (2023). Crystallinity of side-chain fatty acid containing block copolymers with polyisobutylene segment. *European Polymer Journal*, *187*, 111879. http://dx.doi.org/10.1016/j.eurpolymj.2023.111879.

34. Gupta, S., Puttaiahgowda, Y. M., Parambil, A. M., & Kulal, A. (2023). Fabrication of crosslinked piperazine polymer coating: synthesis, characterization and its activity towards microorganisms. *Journal of Molecular Structure*, *1274*(Pt 2), 134522. http://dx.doi.org/10.1016/j.molstruc.2022.134522.

35. ASTM International – ASTM. ASTM F756-17 - Standard Practice for Assessment of Hemolytic Properties of Materials. USA: ASTM International; 2017.